**WOOD RESEARCH** doi.org/10.37763/wr.1336-4561/68.2.208223
**ISSN 1336-4561 e-ISSN 2729-8906**
**68(2): 2023 208-223 pp.**

# EVOLUTION AND DISTRIBUTION OF SHAKES IN LARCH LOGS DURING AIR DRYING

SIDONG WANG, FENGHAO ZHANG, DONGSHENG CHEN, JINGHUI JIANG
CHINESE ACADEMY OF FORESTRY
CHINA

(RECEIVED DECEMBER 2022)

## ABSTRACT

This paper analyzed the length, width, and location of shakes in the air-drying process of larch log (*Larix principis-rupprechtii* Mayr) 1 m long and 66% initial moisture content. The development law and distribution characteristics of shakes during log drying of larch were studied and shake generation and development law were analyzed from two aspects of microstructure and growth defects. The variation of dry shrinkage deformation along the radial direction and knot influence on it was analyzed using the split-shaped stress test strips. At the cellular level, the cell wall shrinkage behavior of heartwood and sapwood and the microstructure of knots were observed. The results showed a significant relationship between eccentricity and shake distribution; the IIa region is the most prone to dry shake. The evolution of shakes is closely related to the drying rate. In the high-speed drying stage (MC ≥ 40%), shakes almost do not occur; in the decelerating drying stage (40% ≥ MC ≥ 20%), the amount, length, and width of shakes increase rapidly. In the low-speed drying stage (20% ≥ MC), the area of shakes tends to stabilize or even decline. The main reasons for dry shaking are the dry shrinkage difference between tangential and radial cell walls, early and late wood, heartwood and sapwood, and moisture content gradient during the drying process.

KEYWORDS: Larch log, air-drying, evolution of shakes, eccentricity, knot.

## INTRODUCTION

Huabei larch (*Larix principis-rupprechtii* Mayr) is widely distributed in Inner Mongolia and North China. It has the advantages of rapid growth, resistance to disease and rot, and high compressive and bending strength (Shao et al. 2011, Kotásková et al. 2016). Larch log is widely

used in construction and as electric poles, but its large shrinkage coefficient and dry defects hinder its high quality and efficient utilization (Jiang 2000).

In the process of log drying, the dry shrinkage cannot be performed freely due to internal unit uneven shrinkage (Yin and Liu 2021), leading to drying stress. Shakes are generated when the drying stress is greater than the wood structure's strength. During the logs' drying process, the logs' surface layer shrinks before the heartwood due to the radial moisture content gradient, which results in tensile stress on the surface (Yu and Wang 2005). In general, the shrinkage rate in tangential direction is higher than that in radial direction, therefore the tangential shrinkage cannot be carried out freely. The dry shrinkage rate of thick-walled cells and wood parenchyma cells (Hao et al. 2021), heartwood and sapwood (Flæte et al. 2000), and juvenile and mature wood (Wang 2022, Mathilde et al. 2010) are different, which limits the free dry shrinkage among tissues. In addition, eccentricity and knot will affect not only the uniformity of wood shrinkage, but also the strength (Liu et al. 1981, Takeda and Hashizume 1999).

In addition to the drying stress, the structural site that first initiates failure when subjected to external action is also an important factor in analyzing the evolution and distribution of shakes (Wang et al. 2022). Compound middle lamella fracture is easier at the cellular level than cell wall fracture during tensile shake propagation (Ren et al. 2008). The tracheid and boundary of early wood and late wood can delay the shake development, and the tensile modulus, tensile strength, and elongation at the break of the latewood tracheid were higher than that of early wood tracheid (Xing et al. 2013). At the tissue level, the area and number of knots were closely related to the tensile strength (Takeda et al. 1999). There was a linear relationship between the growth ring width and latewood percentage and the bending strength and tensile strength, respectively, and the mechanical properties of heartwood are weaker than that of sapwood (Wang et al. 2022). The end surface shake was the mainly form in the early drying stage, and the shake developed to the maximum within the initial 3-4 hours, and then began to gradually recover (Liu et al. 2016). The higher the juvenile wood content, the more serious the dry deformation would be (Chen et al. 2010).

To suppress the dry defects in the drying process, many wood drying quality improvement research based on physical methods has been conducted and a series of pretreatment methods have been proposed, including mechanical pretreatment with kerf/center drilling (Chu et al. 2022, Zhao et al. 2019), steam blasting pretreatment (Torgovnikov and Vinden 2010, Weng et al. 2021), and humid heat pretreatment (Liu et al. 2017, Moya and Tenorio 2022, Zhan and Avramidis 2017). However, there is a lack of influence of growth defects such as knot and eccentricity on shake in relevant studies, and feedback optimization of the pretreatment process through the shake evolution process, which is only evaluated from the perspective of final drying quality. In this experiment, the air-drying quality was evaluated, the distribution and evolution law of dry shakes in larch logs were analyzed, and the effect of knots on wood drying shrinkage was evaluated by stress strips with moisture content gradient excluded. The dry shrinkage behavior of the heartwood and sapwood cells of Huabei larch was observed and described.

## MATERIAL AND METHODS

Nine logs of Huabei larch (*Larix principis-rupprechtii* Mayr) 23-28 years old, 1 m long, 14-16 cm in diameter, with an average initial moisture content of 65.77% were sampled from the Wangyedian plantation in Inner Mongolia. Samples were air-dried at the Physical Research Laboratory of Wood Industry Research Institute, Chinese Academy of Forestry, Beijing, China. The air-drying time was from April 20 to July 13, a total of 113 days, during which the average temperature was 21□ and the average humidity was 48%.

### Test moisture content statistics

Before drying, a 2 cm thick wood disk was sawed 10 cm away from the end of the log, and the moisture content of the disk was measured as the initial moisture content of the log sample. Logs are weighed during the drying process and the moisture content during the drying process is recorded and calculated relative to the initial moisture content.

### Calculation method of log shake area

During the drying process, logs produce side shakes due to moisture content gradient and differential shrinkage. During the drying process, the length, width, and position of the shake with a width greater than or equal to 1 mm were recorded. Shake is usually thick in the middle and thin on both sides (surface shake) or triangular (heart shake), so the shaking area formula is used to estimate and calculate the shake ratio (Eqs. 1, 2).

$$S=\frac{wl_x}{2^k} \quad (1)$$

$$f=\frac{S}{\Pi R l_0} \quad (2)$$

where: S - the approximate area of the shake ($mm^2$), w - the width of shake (cm), $l_x$ - the length of fracture (mm), k - the parameter of shake length (0 - when the shake runs through the side of the log, and 1 – otherwise), f - the shake ratio, R - the diameter of the log end face, and $l_0$ – the length of the log.

### Statistical method of shake location

To explore the influence of eccentricity and knot on shake distribution, the shake location was recorded according to the relative location of the knot and pith. The method of dividing areas according to eccentricity is shown in Fig. 1a.


*a)* *b)* *c)* *d)*

*Fig. 1: a) The partition diagram of log eccentricity, b) the diagram of the log node partition, c) sampling diagram of moisture content gradient sample, d) stress test strips.*

Vertical lines were drawn on the end face using the pith as the center to divide the log into 4 regions. The region which bark is nearest to the pith is Ia, the opposite region to Ia is region IIa, and the rest is region IIIa. The method of dividing areas according to knot is shown in Fig. 1b. The samples were partitioned according to the knot. The knots are in the Ib region, the one-fold knot diameters of the left and right knots are IIb region, and the remaining areas are IIIb regions. The knots in the log can be divided into sound, rotten, and hollow knots. Since all knots in the test material are sound knots which account for the main part of the stumpage knots, this experiment only takes sound knots as the research object.

**Moisture content gradient measurement**

After drying, the tree disks 2 cm thick were sawed 20 cm from the end face. The moisture content gradient samples (2×5 cm) were split along the radial direction on the tree disk (Fig. 1c). The moisture content of the samples was measured.

**Simulation of drying strain caused by the variability of drying shrinkage**

To analyze the areas prone to dry shrinkage stress on the log and evaluate the variation of dry shrinkage strain along the radial direction and the effect of knots on dry shrinkage when the effect of moisture content gradient is excluded, the tree disks 10 mm thick were sawed from the raw logs with and without knots. The stress test strips were split and numbered (Fig. 1d). The samples were air dried and the deflection of various strips calculated as shown in Eq. 3:

$$\gamma = \frac{h\alpha}{l} \quad (3)$$

where: γ is deflection, h is the bending height of the sample and l is the sample span, and α is the direction coefficient, such as the sample test strip along the direction of the number of bending, the deflection is recorded as positive, vice it's negative.

**Determination of tracheid shrinkage characteristics of Huabei larch**

A wood disk 10 mm thick was sawed at the end of the log, and 5×5 mm samples were split at the heartwood and sapwood, respectively. The samples were immersed in water until green, and the semi-automatic slide-away slicer was used to smooth the surface. The cell wall morphology was recorded with a Keenes ultra depth of field 3D microscope, and the microscope observation area was marked by blade scratches. Then the samples were placed in an atmospheric environment until the weight was stable, that is, the air-dry state. The previously marked area was observed and photographed again. The images were imported into ImageJ to measure the thickness of the cell wall and calculate the dry shrinkage rate.

## RESULTS AND DISCUSSION

**Air drying rate and drying quality of Huabei larch logs**

The average initial and final moisture content of logs was 65.77% and 13.88% respectively. The drying time was 90 days, and the average drying rate was 0.58% per day. When

the moisture content is greater than 30%, the drying rate is faster, and the average drying rate is 2.16%/d. When the moisture content is 30%, it enters the slow drying stage, and when the moisture content is about 15%, it enters the low drying stage, during which the average drying rate is 0.48%/d (Fig. 1). Moisture content can be observed two main forms of water, namely free water and bound water (Engelund et al. 2013). When a tree loses all free water, the fiber saturation point (FSP) is reached, which corresponds to a moisture content of 25% to 30%. The drying rate decreases when the moisture content drops below the FSP as for the interactions of bound water and hydrophilic wood polymers (Engelund et al. 2013).

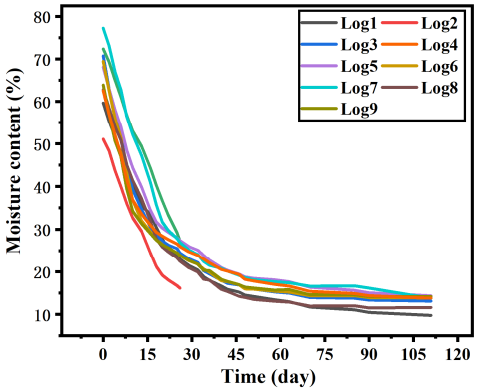


*Fig. 2: Drying curves for the logs studied.*

Shakes with widths greater than or equal to 1 mm were recorded. After air drying, there are some short cracks in the log sample, which have less influence on the drying quality than the long cracks. When the number of air-drying cracks is small, short cracks can make indicators such as average length and average width lose their significance. Therefore, only the shake with a length greater than or equal to 10 cm was statistically analyzed.

The average air-dry shake rate of Huabei larch logs is 1.50%, and the variability of dry quality is large. The shakes number and average length and width vary greatly. Many factors such as moisture gradient, density and diameter can influence wood drying behavior and concequently cause the apperance of shakes (Hornburg et al. 2012, Zanuncio et al. 2015). Knowing the size, amount and distribution of shakes could support the drying stress analysis to develop more effective drying schedules. The logs can be divided into three categories according to the drying quality (Tab. 1): *1)* The number of shakes is small, but the length and width of shakes are large. The drying stress is locally concentrated during the drying process. For example, on average, for No. 6, 7, 9, and 10 logs, the shake rate is 1.15%. *2)* The number, width, and length are large, indicating large drying stress and poor drying quality. For example, the average shake rate of No. 1, 3, 5, and 8 logs is 2.08%. *3)* The shakes are scattered, moderate in quantity and small in width, indicating uniform drying stress and good drying quality. However, the number of such samples is small. For example, No.2 log, the shake rate is 0.58%.

*Tab. 1: Log drying quality.*

| Log number | Diameter (cm) | Number of shakes | Mean shake length (cm) | Mean shake width (cm) | $S$ (cm$^2$) | $f$ (%) |
|---|---|---|---|---|---|---|
| 1 | 13.31 | 10 | 34.32 | 0.34 | 68.33 | 1.82 |
| 2 | 13.21 | 7 | 25.89 | 0.23 | 21.55 | 0.58 |
| 3 | 13.36 | 7 | 44.97 | 0.41 | 75.31 | 1.99 |
| 4 | 13.25 | 3 | 50.93 | 0.29 | 28.70 | 0.77 |
| 5 | 14.24 | 10 | 42.89 | 0.34 | 78.94 | 1.96 |
| 6 | 13.66 | 2 | 58.05 | 0.88 | 52.81 | 1.37 |
| 7 | 12.36 | 5 | 36.76 | 0.45 | 52.37 | 1.50 |
| 8 | 12.05 | 14 | 35.49 | 0.36 | 85.93 | 2.53 |
| 9 | 12.74 | 4 | 35.3 | 0.52 | 35.34 | 0.98 |

Note: Only shakes ≥ 10 cm in length were counted.

At the initial drying stage, with the decrease of moisture content, tensile stress is first generated on the log surface, and then transformed into compressive stress (Li and Lee 2004). Drying stresses is the main cause of the shakes because it can exceed the strength of this material (Kang and Lee 2004). It has been clearly known that the inhomogeneous distribution of moisture within wood resulting moisture content gradient would lead to internal stress (Baettig et al. 2006). Therefore, it is necessary to combine the analysis of water migration and fracture evolution. In the drying process, the moisture distribution along the radial direction remained almost uniform (Kang et al. 2004). The radial moisture content gradient of air-dry Huabei Larch was small, the core layer was 2.41% higher than the surface layer, and the average variance was 0.96. The local fluctuation of moisture content of a few logs is greater than that of the rest, resulting in more cracks (Fig. 3). For example, the radial moisture content of No.1, 3, 5 log fluctuates greatly, and the fracture rate is 77.13 cm$^2$, and the average shake area of the other 5 logs is 38.15 cm$^2$ (Tab. 1).

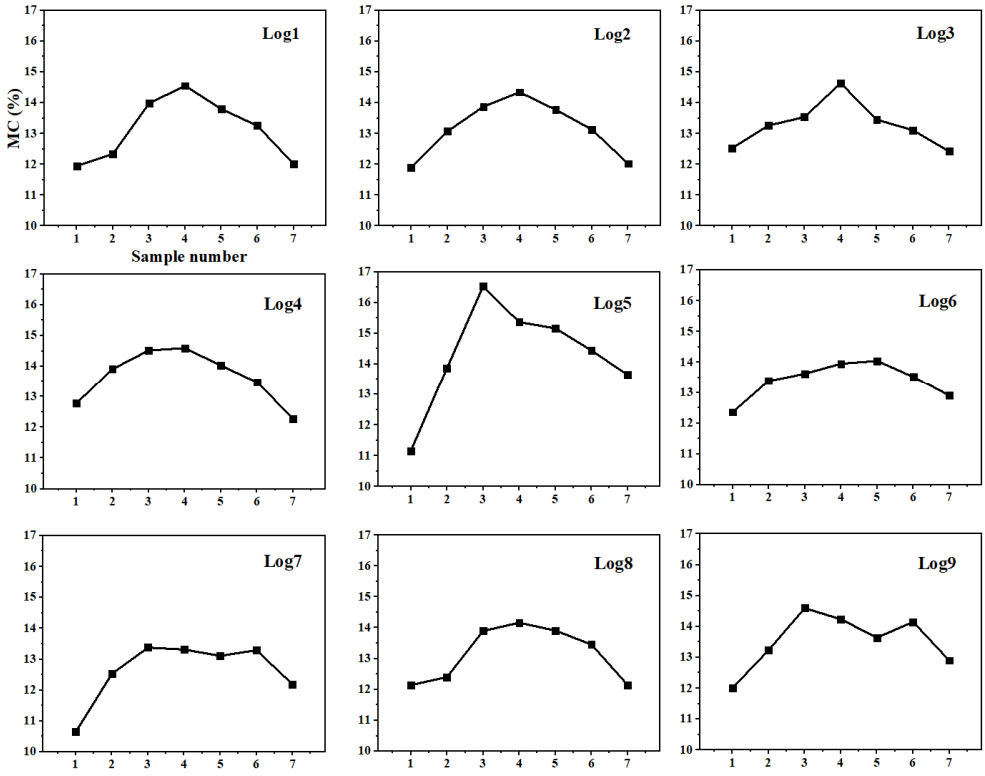


*Fig. 3: The distribution of the final moisture content.*

**Evolution of shakes in larch logs during air drying**

The development of shakes with moisture content can be divided into three stages (Fig. 4). In the initial drying stage (MC ≥ 40%), almost no shakes occurred. The excluded water was mainly free water in the cell lumen and the water content in cell wall does not change significantly until lumen water is depleted (Lamason et al. 2017). In the rapidly decreasing drying rate (MC 40-15%), from sapwood to heartwood, wood moisture content gradually drops below the fiber saturation point, and sapwood cracks rapidly under the action of stress. In the later drying period (moisture content below 15%), the heartwood moisture content decreases below the fiber saturation point. At this time, the heartwood shrinkage occurred and the surface shakes remained stable.

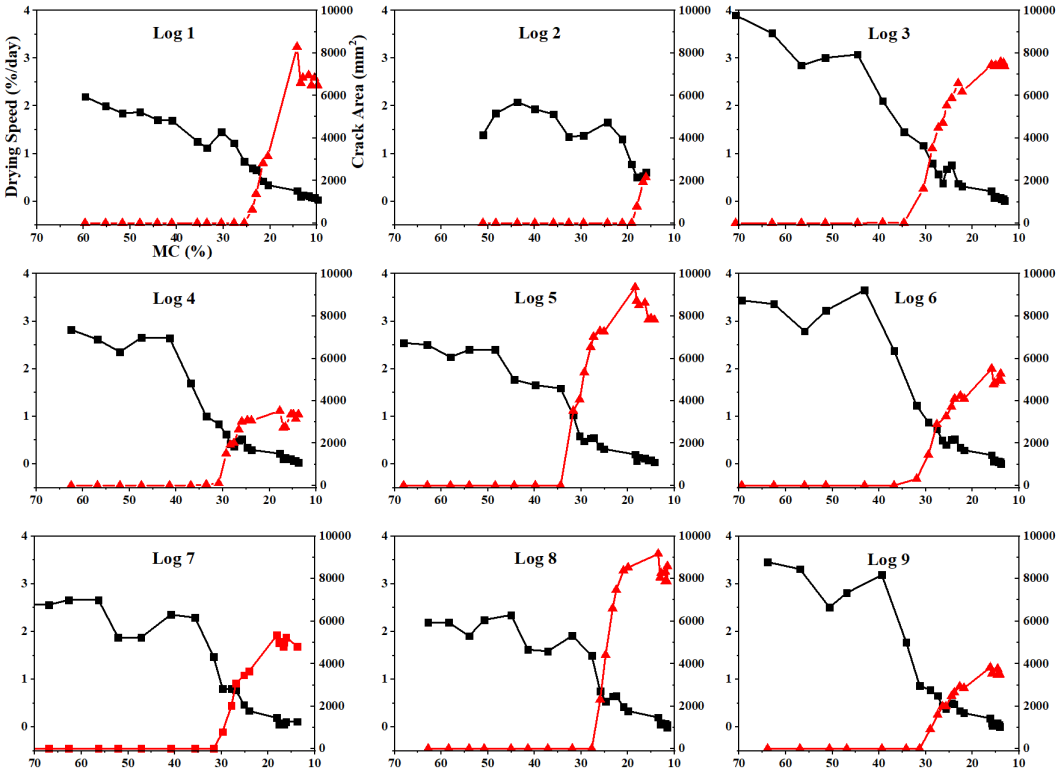


*Fig. 4: Evolution of lateral shake and drying rate of logs.*

To analyze the changes in the number, length, and width of shakes in logs with different moisture content, the crack indexes of 9 logs at the initial cracking stage (MC = 30%), the crack expansion stage (MC = 21%), and the end of drying (MC = 13%, Fig. 6) were statistically analyzed (Fig. 5).

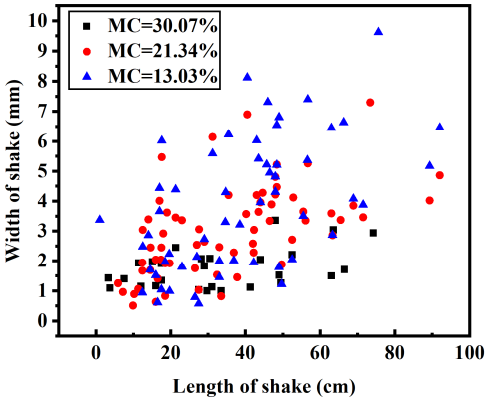


*Fig. 5: Variation of shake length and width with moisture content.*

The number, length, and width of cracks differ by drying stages (Fig. 5). When the moisture content was 30.07%, the shakes were in the generation stage, the number of shakes was low, and the width and length were small. The expansion stage of shakes occurs at 30.07 - 21.34% moisture content. At this stage, the number, width and length of shakes increase. When the moisture content is 21.34 - 13.03%, the number and length of shakes do not change greatly, but the width increases.

Eccentric growth is usually associated with reaction wood and differs in chemical composition, microfilament angle and mechanical property from the normal wood (Rodrigues et al. 2000). Therefore, the response of different regions on the cross section to drying stress is different. According to Fisher's mean test, the results of ANOVA showed that at the 0.05 level, the average shake rate of Ia, IIa, and IIIa was 1.06%, 2.53%, and 1.04%, respectively. The mean shake rate of IIa was significantly higher than in Ia and IIIa, and Ia and IIIa were not significantly different. Region IIa is more likely to produce a dry shake phenomenon. Among all samples, the shake rate in region Ia is the lowest (Tab. 2).

*Tab. 2: Statistical table of fracture distribution according to eccentric region.*

| Log number | Rate of eccentricity | Region | Area of shake ($cm^2$) | Area of region ($cm^2$) | Ratio of shake (%) | Area of knot region ($cm^2$) | | |
|---|---|---|---|---|---|---|---|---|
| | | | | | | Ib | IIb | IIIb |
| | | $I_a$ | 14.80 | 846 | 1.75 | 0 | 0 | 846 |
| 1 | 0.49 | $II_a$ | 25.90 | 1062 | 2.44 | 270 | 540 | 252 |
| | | $III_a$ | 32.97 | 1899 | 1.74 | 0 | 0 | 1899 |
| | | $I_a$ | 1.51 | 912 | 0.16 | 630 | 282.6 | 0 |
| 2 | 0.43 | $II_a$ | 15.11 | 989 | 1.53 | 0 | 0 | 989.1 |
| | | $III_a$ | 6.30 | 1897 | 0.33 | 0 | 887.4 | 1009.8 |
| | | $I_a$ | 5.55 | 972 | 0.57 | 270 | 270 | 432 |
| 3 | 0.42 | $II_a$ | 21.95 | 990 | 2.22 | 180 | 360 | 450 |
| | | $III_a$ | 35.81 | 1899 | 1.89 | 180 | 630 | 1089 |
| | | $I_a$ | 0.00 | 900 | 0.00 | 90 | 180 | 630 |
| 4 | 0.27 | $II_a$ | 1.45 | 945 | 0.15 | 90 | 180 | 675 |
| | | $III_a$ | 13.83 | 1845 | 0.75 | 0 | 0 | 1845 |
| | | $I_a$ | 4.78 | 981 | 0.49 | 0 | 0 | 981 |
| 5 | 0.24 | $II_a$ | 24.40 | 990 | 2.46 | 0 | 0 | 990 |
| | | $III_a$ | 53.92 | 2034 | 2.65 | 0 | 0 | 2034 |
| | | $I_a$ | 0.00 | 855 | 0.00 | 360 | 414 | 36 |
| 6 | 0.57 | $II_a$ | 52.81 | 1098 | 4.81 | 180 | 180 | 738 |
| | | $III_a$ | 0.00 | 1899 | 0.00 | 0 | 846 | 1053 |

| | | | | | | | | |
|---|---|---|---|---|---|---|---|---|
| | | $I_a$ | 20.98 | 981 | 2.14 | 0 | 135 | 846 |
| 7 | 0.47 | $II_a$ | 28.74 | 990 | 2.90 | 0 | 90 | 900 |
| | | $III_a$ | 2.65 | 1881 | 0.14 | 405 | 585 | 891 |
| | | $I_a$ | 31.55 | 810 | 3.89 | 0 | 0 | 810 |
| 8 | 0.40 | $II_a$ | 38.15 | 783 | 4.87 | 0 | 0 | 783 |
| | | $III_a$ | 16.23 | 1710 | 0.95 | 495 | 990 | 1485 |
| | | $I_a$ | 5.30 | 873 | 0.61 | 270 | 360 | 243 |
| 9 | 0.33 | $II_a$ | 12.61 | 936 | 1.35 | 0 | 135 | 801 |
| | | $III_a$ | 17.43 | 1890 | 0.92 | 270 | 495 | 1125 |

Except for No. 5 and 10 logs, the shake rate in Region IIa is the highest, indicating that the drying quality in region Ia is the best and the logs in region IIa are the most severely fractured. The eccentricity of the No. 5 log is small, and there is no knot. The dry shake may be affected by other factors, such as texture and growth defects, which need further exploration. The eccentricity of the No.10 log is low; therefore, the dry shake is less affected by eccentricity, and may be more affected by the knot distribution. Region IIIa of No. 10 log is all knot subdivision IIIb. All shakes of the No. 10 log are in region IIIb (Tab. 3). The relationship between shake distribution and the knot is not significant, which is inferred to be caused by the shake distribution being more affected by eccentricity than by the knot. However, overall, the average shake rate in Regions Ib, IIb, and IIIb is 0.94%, 1.33%, and 1.56%, respectively, which seems that region IIIb is relatively easy to shake.

*Tab. 3: Shakes distribution in knot region.*

| **Log number** | **Number of knots** | **Region** | ***S*** **(cm$^2$)** | **Region area (cm$^2$)** | ***f*** **(%)** |
|---|---|---|---|---|---|
| | | $I_b$ | 2.88 | 540 | 0.53 |
| 1 | 1 | $II_b$ | 37.20 | 1080 | 3.44 |
| | | $III_b$ | 28.25 | 2187 | 1.29 |
| | | $I_b$ | 1.28 | 630 | 0.20 |
| 2 | 3 | $II_b$ | 5.17 | 1170 | 0.44 |
| | | $III_b$ | 12.61 | 1980 | 0.64 |
| | | $I_b$ | 12.96 | 630 | 2.06 |
| 3 | 3 | $II_b$ | 16.83 | 1260 | 1.34 |
| | | $III_b$ | 45.52 | 1971 | 2.31 |
| | | $I_b$ | 0.00 | 180 | 0.00 |
| 4 | 1 | $II_b$ | 0.00 | 360 | 0.00 |
| | | $III_b$ | 28.70 | 3150 | 0.91 |
| | | $I_b$ | 0.00 | 0 | 0 |
| 5 | 0 | $II_b$ | 0.00 | 0 | 0 |
| | | $III_b$ | 78.94 | 4005 | 1.97 |
| | | $I_b$ | 0.00 | 765 | 0.00 |
| 6 | 3 | $II_b$ | 16.44 | 1530 | 1.07 |
| | | $III_b$ | 36.36 | 1710 | 2.13 |
| | | $I_b$ | 5.96 | 405 | 1.47 |
| 7 | 2 | $II_b$ | 5.96 | 810 | 0.74 |
| | | $III_b$ | 40.44 | 2538 | 1.59 |
| | | $I_b$ | 13.13 | 405 | 3.24 |
| 8 | 2 | $II_b$ | 15.64 | 810 | 1.93 |
| | | $III_b$ | 57.16 | 2088 | 2.74 |
| | | $I_b$ | 0.00 | 540 | 0.00 |
| 9 | 1 | $II_b$ | 17.91 | 1080 | 1.66 |
| | | $III_b$ | 17.43 | 2079 | 0.84 |

The variation curve of the knot-free sample shows an "S" shape (Fig. 6), the bending direction changes at pith, and the deflection changes the most, which explains the characteristics of the fracture radial distribution in the cross-section of the log during the drying process.

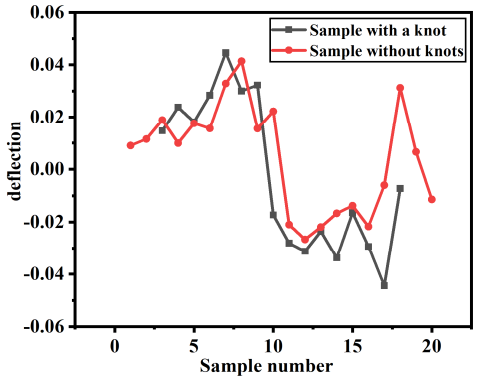


*Fig. 6: Variation of dry shrinkage deflection of the air-dry stress test strip.*

The stress strip variation of heartwood and sapwood is different, which may related to their texture and dry shrinkage characteristics. The variation curve of the knot sample shows an “M” shape (Fig. 6). No. 12-16 stress strips are knots in the sample. The knot impacts the texture of the No. 17-20 samples (Fig. 1). This indicates that during the log drying, the knot will damage the continuity of the stringed shrinkage strain distributed along the growth ring.

**Evaluation of dry shrinkage characteristics of Huabei larch**

When the sample used to observe microstructure size is small (5×5×10 mm) and the drying method is air dry, the influence of drying stress caused by moisture content gradient on cell shape can be ignored. The morphological changes before and after cell shrinkage can be attributed to the differences in cell-cell shrinkage (Fig. 7). In addition, the average thickness of earlywood cells (2.88 μm) and latewood (7.69 μm cells) might be related to different failure modes. The cell wall in the earlywood region is relatively thin, mainly due to cell wall breakage. Due to the relatively thicker cell wall in the latewood region, the intercellular layer is destroyed (Ren et al. 2008).

Drying stress depended significantly on themechanical interaction between early and late wood due to the difference of drying shrinkage (Watanabe et al. 1998). The morphological difference of latewood cells before and after drying was mainly in size while the shape of earlywood cells changed greatly (Fig. 7).

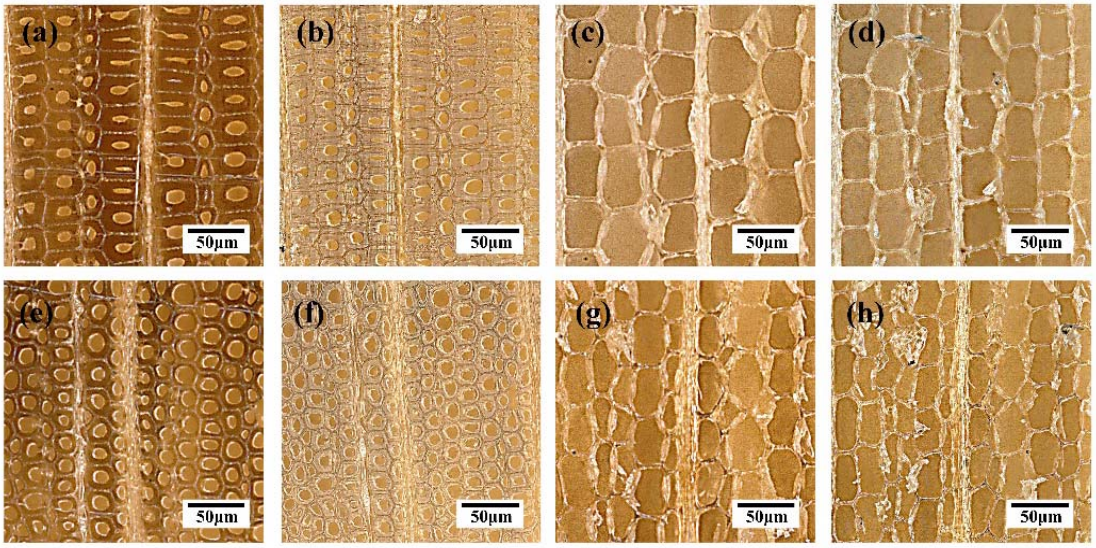


*Fig. 7: a) the green late sapwood; b) the air-dry late sapwood; c) the green early sapwood, d) the air-dry early air-dry sapwood, e) the green late heartwood, f) the air-dry late heartwood, g) the green earlywood heartwood, and h) the air-dry early heartwood.*

The shape changes of the earlywood cells of sapwood were small before and after drying. In contrast, the earlywood cells of heartwood showed large deformation after air drying (Fig. 7). The cell shape changes due to its anisotropic dry shrinkage and the drying stress caused by the difference in dry shrinkage with the surrounding cells. The reasons are speculated to be two aspects. First, the drying shrinkage rate of the tangential and radial walls is greater in early heartwood cells than in sapwood, and deformation is more likely to occur during the drying shrinkage process. Second, the shrinkage difference between the earlywood and latewood is greater in heartwood than in sapwood, and the drying stress in its growth ring is greater. Latewood has a thick cavity and a lower drying shrinkage rate than earlywood (Tab. 4), which distributes on both sides of the earlywood band and can limit its drying shrinkage. Due to the thin cell wall and poor mechanical properties of earlywood, shakes occur mostly at the earlywood or the junction of earlywood and latewood, in the actual drying process (Hao et al. 2021, Enhua 2018).

*Tab. 4: Cell wall shrinkage of heartwood and sapwood of Huabei larch.*

| Sampling position | Direction of cells | MC | Thickness (μm) | SD | Amount | Shrinkage (%) | Differential shrinkage coefficient |
|---|---|---|---|---|---|---|---|
| Sapwood/Latewood | Radial wall | Green | 9.57 | 1.68 | 52 | 23.88 | 1.60 |
| | | Air-dry | 7.73 | 1.03 | 54 | | |
| | Tangential wall | Green | 12.16 | 1.53 | 54 | 38.27 | |
| | | Air-dry | 8.79 | 1.47 | 54 | | |
| Sapwood/Earlywood | Radial wall | Green | 3.02 | 0.43 | 21 | 40.68 | 1.01 |
| | | Air-dry | 2.15 | 0.20 | 22 | | |
| | Tangential wall | Green | 4.54 | 0.98 | 19 | 41.07 | |
| | | Air-dry | 3.21 | 0.75 | 20 | | |
| Heartwood/latewood | Radial wall | Green | 5.91 | 1.01 | 51 | 5.13 | 1.74 |
| | | Air-dry | 5.62 | 0.85 | 51 | | |
| | Tangential wall | Green | 6.10 | 0.82 | 52 | 8.93 | |
| | | Air-dry | 5.60 | 1.14 | 51 | | |

| | | | | | | | |
|---|---|---|---|---|---|---|---|
| Heartwood/Earlywood | Radial wall | Green | 2.82 | 0.43 | 28 | 69.20 | 0.82 |
| | | Air-dry | 1.66 | 0.30 | 27 | | |
| | Tangential wall | Green | 3.43 | 0.84 | 22 | 56.24 | |
| | | Air-dry | 2.19 | 0.86 | 21 | | |

The difference between actual and free drying shrinkage is the key factor in determining the drying stress direction (Tu and Liu 2009). The differential shrinkage coefficient between early and late wood will lead to drying stress in the growth ring (Yu and Wang 2005). The cell drying shrinkage rate of early sapwood was 1.32 times that of late sapwood, and the drying shrinkage rate of early heartwood was 8.92 times that of late heartwood (Tab. 4). There was compressive stress in latewood and tensile stress in earlywood, and the stress of heartwood was greater than that of sapwood because of restraining effect of latewood on earlywood (Patera et al. 2018). The earlywood cell wall is thin, the mechanical properties are poor, and the cell structure is easily deformed or damaged when the inner stress is large (Watanabe et al. 2000). The tangential shrinkage rate of late sapwood cells was 4.29 times that of the heartwood tangential wall (Tab. 4). The difference in tangential shrinkage between heartwood and sapwood resulted in drying stress, sapwood tensile stress, and heartwood compression stress. For sapwood and heartwood, the average difference rate of tangential and radial dry shrinkage was 1.67 (Tab. 4), and tangential dry shrinkage was inhibited. On the cross-section of the log, the differential shrinkage of the tangential and radial walls caused tangential drying stresses.

There are shakes around the knot and between the knot and the surrounding tissues (Fig. 8b,c), with widths of about 15.33 μm and 32.12 μm, respectively, providing space for deformation. It can conducive to the drying stress release. Knots impact the texture of the surrounding tissues (Fig. 10c). Comparison of Fig. 8f and Fig. 7 shows an evident difference between the arrangement of knot cells and the cells of non-knot tissues. The disorder texture of surrounding knot tissues, the structure of the knot itself, and the morphology of cells disrupt the arrangement of wood cells. This may reduce the stress caused by differential tangential and radial shrinkage based on wood texture.

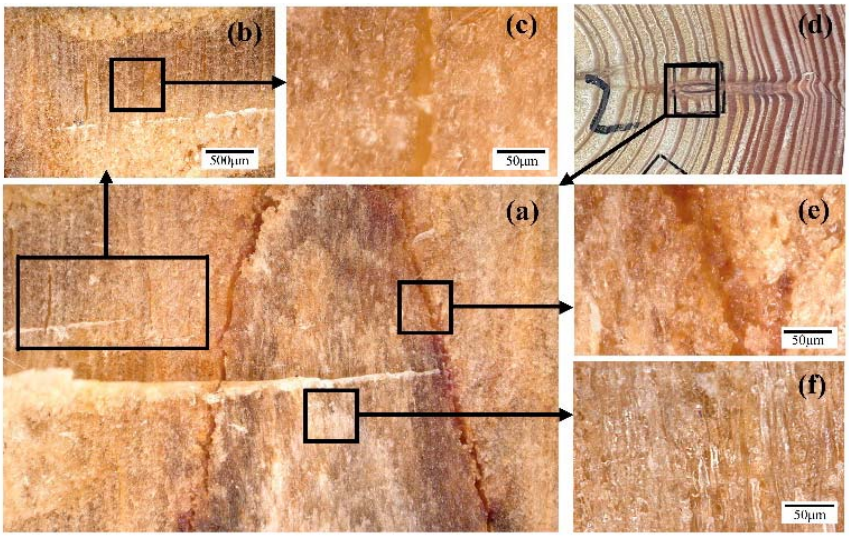


*Fig. 8: a) Knot microstructure, b) cracks around a knot, c) part of a crack around a knot, d) kodes and surrounding tissues, e) the gap between the node and the surrounding tissue, and f) knot cells.*

## CONCLUSIONS

The air-dry mass variability of larch wood was large, the average shake rate was 1.50%, and the average moisture content difference between heartwood and sapwood was 2.41%. There are three stages in the drying process, namely constant drying (MC ≥ 40%), slow drying (40% MC ≥ 15%), and low drying (15% MC ≥ 15%), with the average drying rate being 2.42%/ day, 0.57%/ day, and 0.05%/ day, respectively. The shake evolution of logs is closely related to the moisture content. There is almost no shake when the moisture content is above 40%. At 40-15% moisture content, the number, length, and width of shakes increase rapidly. When the fracture is lower than 15%, it almost stops expanding and tends to be stable or decrease slightly. The distribution relationship between eccentricity and shake is significant, and the eccentricity of region IIa is the most prone to dry shake.

The change rate of strain caused by dry shrinkage anisotropy at the pulp center was the largest, and the dry shrinkage strain law in and around the node significantly differed from that in the region without defects. Due to the shrinkage differences between earlywood and latewood cells, the heartwood and sapwood, and the tangential and radical cell wall, the growth rings between heartwood and sapwood and the drying stresses in the cross-section will be generated in the tangential direction during the drying process. Moisture content gradient also causes drying stress.

## ACKNOWLEDGMENTS

We would like to thank the National Science Foundation of China (Grant number 31971652) for providing financial support for the research.

## REFERENCES

1. Baettig R., Rémond R., Perré P., 2006: Measuring moisture content profiles in a board during drying: A polychromatic X-ray system interfaced with a vacuum/pressure laboratory kiln. Wood Science and Technology 40(4): 261-274.
2. Chen, T.A., Wang, Y.X., Pang, S.S., 2010: Analysis of drying distortion of plantation Douglas-fir structural lumber. China Wood Industry 24(6): 33–35.
3. Christoforo, A.L., Almeida, T.H.D., Almeida, D.H.D., Santos, J.C.D., Panzera, T.H., Lahr, F.A.R., 2016: Shrinkage for some wood species estimated by density. International Journal of Materials Engineering 6(2): 23-27.
4. Chu, J.Y., Wang, S.D., Jiang, J.H., Wang, Z.H., 2022: Effects of mechanical pretreatment on the conventional drying characteristics of larch logs. Journal of Central South University of Forestry and Technology 42(4): 162–69.
5. Clevan, L., Bryce M., Bruce B., Brigitte L., Zarin P., 2017: Magnetic resonance studies of wood log-drying processes. Forest Products Journal 67(3-4): 266–274.
6. Enhua, X., 2018: Properties and chemical composition distribution of wood cell walls. Wood Research 63(2): 179-192.

7. Engelund, E.T., Thygesen, L.G., Svensson, S., Hill, C.A.S., 2013: A critical discussion of the physics of wood–water interactions. Wood Science Technology 47(1):141-161.
8. Flæte, P.O., Høibø, O.A., Fjærtoft, F., Nilsen, T.N., 2000: Crack formation in unfinished siding of aspen (*Populus tremula* L.) and Norway spruce (*Picea abies* (L.) Karst.) during accelerated weathering. Holz als Roh- und Werkstoff 58(3): 135–139.
9. Hao, X.F., Xu, K., Li, X.J., Qiao, J.Z., Wu, Y.Q., 2021: Study on the stress evolution mechanism of wood drying based on micromechanics. China Forest Products Industry 58(6): 1-6+20.
10. Hornburg, K.F., Eleotério, J.R., Bagattoli, T.R., and Nicoletti, A.L., 2012: Log and lumber quality of six eucalypts species cultivated on the coast of Santa Catarina. Scientia Forestalis 40(96): 463-471.
11. Jiang, F.L., Yu, H.,2000: Discussion on utilization way of larch wood. Forestry Science& Technology 25(2): 55–56.
12. Kang, W., Lee, N. H., 2004: Relationship between radial variations in shrinkage and drying defects of tree disks. Journal of Wood Science 50: 209-216.
13. Kang, W., Lee, N.H., Choi, J.H., 2004: A radial distribution of moistures and tangential strains within a larch log cross section during radio-frequency/vacuum drying. Holz als Roh-und Werkstoff 62: 59-63.
14. Lamason, C., MacMillan, B., Balcom, B., Leblon, B., Pirouz, Z., 2017: Magnetic resonance studies of wood log-drying processes. Forest Products Journal 67(3-4): 266–274.
15. Li, C.Y., Nam H.L., 2004: Effect of compressive load on shrinkage of larch blocks during radio – frequency vacuum heating. Wood and Fiber Science 36(1): 9-16.
16. Liu, H.H., Yang, L., Wu, Z.H., Jiang, T., Li, X.Y., 2017: Effect of vacuum drying set and radio-frequency/vacuum drying on wood quality. Journal of Northeast Forest University 45(2): 61-64.
17. Liu, S.L., Fang, W.B., Li, F.Y.,1981: Study on the influence of Chinese fir knots on bearing capacity of flexural unit. Journal of Central South University of Forestry & Technology 1(1): 22-38.
18. Liu, Y., Huang, T.H., Lu, C.X., Chen, J.B., Xiang, D.Y., 2016: Drying characteristics of juvenile wood of *Eucalyptus urophylla* × *E. grandis*. Eucalypt Science & Technology 33(1): 27-31.
19. Mathilde, L., Clemens, M.A., Leena, V., Michael, C.J., 2010: Wood shrinkage: influence of anatomy, cell wall architecture, chemical composition and cambial age. European Journal of Wood and Wood Products 68: 87-94.
20. Moya, R., Carolina, T., 2022. Reduction of effect growth stress presence using endless screw during kiln drying and steaming and heating treatment in log before sawing. Wood Research 67(1): 157-169.
21. Ren, N., Liu, Y.X., Gong, C.Z., 2008: Relationship between wood microstructure and tensile fracture. Journal of Northeast Forest University 36(2): 33-35.
22. Shao, Y.L., An, Z., Xing, X.T., 2011: Advance on mechanical properties and application of Larix. Wood Processing Machinery 22(3): 46-49+37.

23. Takeda, T., Takeo, H., 1999: Differences of tensile strength distribution between mechanically high-grade and low-grade Japanese larch lumber 11: effect of knots on tensile strength distribution. Journal of Wood Science 45(3): 207–212.
24. Torgovnikov, G., Vinden, P., 2010: Microwave wood modification technology and its applications. Forest Products Journal 60(2): 173–82.
25. Tu, D.Y., Liu, B., 2009: Study on drying stress model of wood. Journal of Nanjing Forestry University 33(3): 87-91.
26. Patera, A., Van den Bulcke, J., Boone, M.N., Derome, D., Carmeliet, J., 2018: Swelling interactions of earlywood and latewood across a growth ring: global and local deformations. Wood Science and Technology 52: 91-114.
27. Kotásková, P., Havířová, Z., Šmak, M., Straka, B., 2016: Log buildings from the perspective of the current requirements. Wood Research 61(4): 615-626.
28. Watanabe, U., Norimoto, M., Fujita, M., Gril, J., 1998: Transverse shrinkage anisotropy of coniferous wood investigated by the power spectrum analysis. Journal of Wood Science 44(1): 9-14.
29. Watanabe, U., Norimoto, M., Morooka, T., 2000: Cell wall thickness and tangential Young's modulus in coniferous early wood. Journal of Wood Science 46: 109-114.
30. Wang, Z.Y., Lin, L.Y., Fu, F., Zhou, Y.D., Li, S.M., Peng, L.M., Yin, S.L., 2022: Research progress on high-intensity microwave treatment and failure mechanism of wood. Journal of Forestry Engineering 7(4): 13-21.
31. Wang, S.D., Chen, D.S., Chu, J.Y., Jiang, J.H., 2022: Effect of growth ring width and latewood content on selected physical and mechanical properties of plantation Japanese larch wood. Forests 13(5): 797.
32. Weng, X., Zhou, Y.D., Fu, Z.Y., Gao, Xin., Zhou, Fan., Jiang, J.H., 2021: Effects of microwave pretreatment on drying of 50 mm-thickness Chinese fir lumber. Journal of Wood Science 67(1):13.
33. Xing, X.T., Shao, Y.L., An, Z., Zhao, R.J., Ren, H.Q., 2013: Mechanical properties of single tracheids of *Larix olgensi* wood. Journal of Anhui Agricultural University 40(4): 597–602.
34. Yin, Y., Liu, H.H., 2021: Drying stress and strain of wood: A Review. Applied Sciences 11(11): 5023.
35. Yu, J.F., Wang, X.M., 2005: The development of macroscopic model on wood drying stress strain. Scientia Silvae Sinicae 41(5): 214-128.
36. Zanuncio, A.J.V., Carvalho, A.G., da Silva, L.F., Lima, J.T., Trugilho, P.F., da Silva, J.R.M., 2015: Predicting moisture content from basic density and diameter during air drying of Eucalyptus and Corymbia logs. Maderas. Ciencia y tecnología 17(2): 335-344.
37. Zhao, X.F., Sun, Y.T., 2019: Effect of inner diameter on drying characteristics of larch center bored round timber during conventional drying. Journal of Beihua University 20(3): 412-415.
38. Zhan, J.F., Stavros, A., 2017: Impact of conventional drying and thermal post-treatment on the residual stresses and shape deformations of larch lumber. Drying Technology 35(1): 15–24.

SIDONG WANG, FENGHAO ZHANG, JINGHUI JIANG*
CHINESE ACADEMY OF FORESTRY
RESEARCH INSTITUTE OF WOOD INDUSTRY
BEIJING, 100091
CHINA
*Corresponding author: Jiangjh@caf.ac.cn

DONGSHENG CHEN
CHINESE ACADEMY OF FORESTRY
RESEARCH INSTITUTE OF FORESTRY
BEIJING, 100091
CHINA